TWENTY-SECOND INTERNATIONAL CONFERENCE ON COMPOSITE MATERIALS (ICCM22)

PROPERTIES OF POLYAMIDE-6 COMPOSITES USING A LOW-COST THERMOPLASTIC RESIN TRANSFER MOULDING SYSTEM

James J. Murray[1], Klaus Gleich[2], Edward D. McCarthy[1], Conchúr Ó Brádaigh[1]

[1] School of Engineering, Institute for Materials and Processes, Sanderson Building, The University of Edinburgh

[2] Johns Manville Europe GmbH, Werner-Schuller-Str.1, 97877, Wertheim, Germany

Keywords: Thermoplastic, In-situ, Reactive, TP-RTM, Polyamide

ABSTRACT

Glass-fibre/Polyamide-6 (GF/PA-6) composite laminates were manufactured using a bespoke, low-cost thermoplastic resin transfer molding (T-RTM) system. Instead of injecting melted fully pre-polymerized PA-6, monomer precursor materials with viscosities ~10mPa.s were injected into a glass-fibre fabric contained between heated platens of a press and polymerisation occurred in-situ within several minutes. Due to the extremely low viscosity of the monomer, composites with fibre volume fractions ~53% with excellent wet-out were produced at a pressure of approximately 4 bar, negating the need for expensive high pressure injection. In this study, the interfacial adhesion of the composite was further improved by using specialized fibre sizings containing one of the chemical reactants such that polymer growth was initiated from the fibre surface. The improved interfacial adhesion resulted in a significant increase in both strength and modulus of the composites in flexure. Fracture surfaces of the failed flexural samples were observed using scanning electron microscopy (SEM) which showed clear signs of improved fibre-matrix interfacial bonding. The void distribution in the laminates was studied using computerised tomography (CT) scans while the fibre volume fraction was determined using burn-off.

1 INTRODUCTION

Engineering and advanced thermoplastic polymers have many desirable properties such as high strength and toughness, and because they can be melted, they can be recycled and welded. Resin transfer moulding (RTM) is one of the most suitable methods for producing small-medium sized parts in large volumes [1]; however, due to the high viscosity of most thermoplastics when melted, they cannot practically be injected into a fibre preform. The development of new methods of producing thermoplastic composites have emerged in recent years [2]–[6]. Rather than melt processing the thermoplastic polymers, the monomer precursor and reactants with significantly lower viscosities can be infused into a mould containing a fibre preform, where polymerisation can occur *in-situ*. One such system takes advantage of anionic ring-opening polymerisation of the ε-caprolactam, a low viscosity monomer, which can be polymerized in-situ to produce APA-6. This work was inspired by a renewed interest in APA-6 for composites as a result of extensive studies carried out by van Rijswijk et al. [3], [7]–[9] involving the development of a system to manufacture wind turbine blades using vacuum infusion and slow reacting catalysts. Since this work, industrial collaborations between automotive companies, resin suppliers and injection system manufacturers have been developing thermoplastic resin transfer moulding (*TP-RTM* or *T-RTM*) processes for the production of parts in large volumes[10]–[12]. It has been reported that Krauss Maffei produced a CF/GF hybrid roadster roof frame with an APA-6 matrix and a fibre volume fraction of ~70% within a 2 minute cycle using TP-RTM with a compression step. Excellent impregnation at high fibre volume fractions are possible at relatively low pressures compared to most thermoset resins, because of the almost water-like viscosity, thus reducing the cost of the injection equipment required. The use of fast-acting catalysts has allowed the reaction to be carried out in cycle times short enough for high volume manufacturing, (ca. 3 min) making it more suitable for the automotive industry.

Ageyava et al. published an in-depth review of polymers and related composites produced from ring-opening polymerisation of lactams in 2018, which summarised relevant work carried out in the field [13]. There are no reports of TP-RTM work carried out on GF/APA-6 composites, and those using VaRTM tend to have void contents that are too high and inconsistent for use in most applications [8]. There is no availability of mechanical test data for unidirectional GF/APA-6 composites, something which is useful for design and finite element modelling. As part of a larger study, which aims to fully characterise all static mechanical properties, this paper focuses on the flexural performance of unidirectional GF/APA-6 composites with a low void content produced using TP-RTM and how this can be achieved by controlling process parameters.

2 METHODOLOGY

2.1 Materials and storage

The polyamide matrix was produced from the following three raw materials: ε-caprolactam monomer, hexamethylene-1,6-dicarbamoylcaprolactam activator/caprolactam blend (BRUGGOLEN® C20p) and sodium-caprolactamate/caprolactam blend (BRUGGOLEN® C10), all kindly provided by Brüggemann GmbH & Co. KG (Heilbronn, Germany). Due to the hydrophilic nature of the precursor materials and the sensitivity of the polymerisation to moisture, special care was given to them in storage, preparation and processing. The materials were stored in air-tight bags contained in a sealed storage drum with desiccant, and a nitrogen purge was used before sealing the drum each time. During preparation, the materials were weighed and in the process were exposed to air, but only for a short period, and then they were stored in jars with silica gel bags.
A 640 g/m^2 unidirectional non-crimp fabric (NCF) with glass fibre rovings was used as the reinforcement material with a filament diameter of ~17μm. The NCF consisted of polyester stitching perpendicular to the fibre direction in 5mm increments. Two different Johns Manville rovings were used in the NCF: StarRov® 871, sized with a standard silane agent; and StarRov® 886 RXN, sized with a reactive agent, which acts as an initiation site to promote polymer chain growth from the fibre surface during polymerisation. The latter enhances interfacial properties, and as a result, the composite properties are improved.

2.2 Thermoplastic resin transfer moulding equipment

The setup for manufacturing laminates consisted of a TP-RTM machine to mix and pump the precursors, a pneumatic press, a closed mould, a vacuum pump and a catch pot as shown in Figure 1 below. The TP-RTM machine consisted of two heated component tanks with stirrers and a set of pumps for each. Each component tank had a recirculation line, which allowed (a) most of the equipment at the mixing head to be heated to the same temperature prior to injection, (b) match flow fronts prior to injection and (c) a protection against deadheading. Each component also had an injection line allowing for the two components to be mixed via a static mixing head prior to entering the mould. Each component had a set of solenoid valves, which were controlled to direct the flow in either the recirculation or injection path. Nitrogen gas was used to purge the component tanks to create an inert atmosphere and was also used to flush the lines before and after injection. All the TP-RTM machine components shown in Figure 1 were contained within a heated enclosure so that a minimum temperature above melt could be maintained at all times. After mixing, the resin exited the machine and was transferred to the mould via aluminum tubing with an in-line pressure sensor to monitor and record the data during injection. A vacuum pump and catch pot were fixed on the outlet side of the mould. The use of a three-way valve on the inlet side with an L-port configuration allowed for drawing of the vacuum while still being able to bleed air between the resin flow front and the vacuum. The cost to build the T-RTM machine was relatively inexpensive (~£5000) and could easily be built in a reasonably short time.

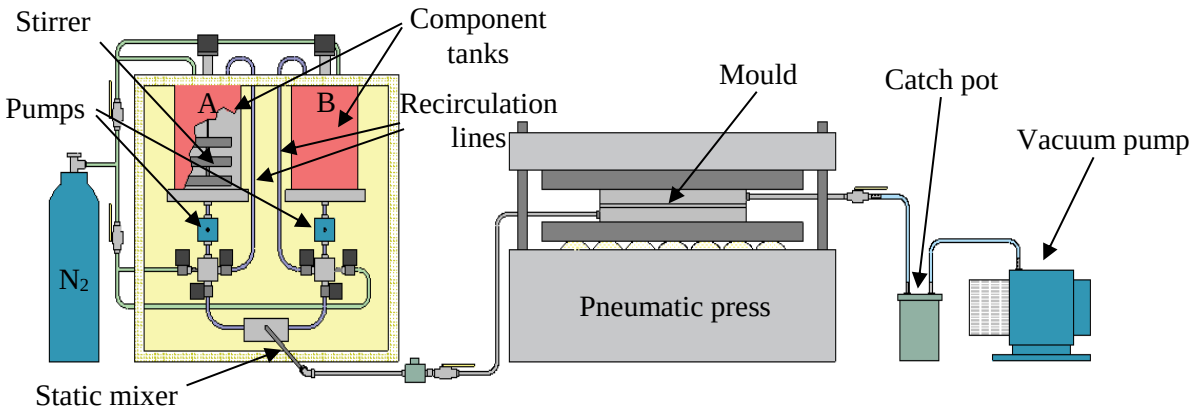

Figure 1: TP-RTM setup consisting of a TP-RTM machine, pneumatic press, closed mould, vacuum pump and catch pot.

2.3 Manufacturing process and preparation

All mould surfaces were cleaned with acetone and two coats of Frekote 55NC mould release agent were applied. All the taps and tubing used to transport the resin were cleaned with hot water at 90°C to dissolve the caprolactam followed by drying at 110°C in air. For composite manufacturing, 350mm x 390mm plies of glass fibre NCF were cut and placed in the mould with the fibres aligned in the bulk flow direction. The mould surfaces were sealed using silicone rubber. A 4mm cavity was used for making pure polymer and a 2mm cavity was used for the composite. The mould was placed between the platens of the press which were heated to 130°C and a vacuum was drawn such that the cavity acted as a vacuum chamber to dry the fibre for at least 90 minutes for each run.

A local tank temperature and a global enclosure temperature of 90°C was used for the component tanks. To further minimise moisture in the system, an initial flush run of the TP-RTM machine was carried out at the start of each day of use by melting a small volume of ε-caprolactam in each tank, recirculating it and injecting it into a bucket. For manufacturing, a mixture of 98.2 mol% ε-caprolactam, 0.6 mol% bi-functional activator and 1.2 mol% catalyst was used. The caprolactam and activator were poured into tank A and caprolactam and catalyst were poured in to tank B such that the volume of resin in each tank was the same, and a nitrogen purge was used. The mould temperature was increased to 160°C for polymerisation having been maintained at 130°C up to this point as only enough heat was required to remove moisture from the fabric, and holding the fabric at a higher temperature over a long time period could result in oxidation of the sizing, although this effect would be decelerated by the partial vacuum. The vacuum was then restricted such that the pressure increased above the vaporization pressure of the mixed resin to prevent boiling in the mould. With an exothermic temperature peak during polymerisation of around 170°C, the pressure below which boiling would occur was 5.3kPa [14]. When a pressure reading of approximately 6kPa was observed on the catch pot gauge, the TP-RTM machine was switched to injection mode using a 820ml/min. flow rate, and when resin exited the bleed port (having bled the air), the valve was rotated to direct the resin flow into the mould. When the resin exited on the outlet side, a valve at the outlet was rotated to reduce the flow and as a result, increase the pressure in the mould to around 4 bars to enhance the wet-out of the fabric by the reacting monomer mixture. The heat was turned off after 15 minutes, and the mould cooled down naturally at ~2.7°C/min.

2.4 X-ray CT scanning

Computerised tomography scans were carried out on 15mm x 15mm specimens taken from 9 different locations on a laminate. Approximately 80 images of each sample were compiled to generate 3D representations such as those in Figure 2 below. The brightness was then adjusted so that greater focus was placed on the areas of interest followed by threshold segmentation to determine the macro void content by volume.

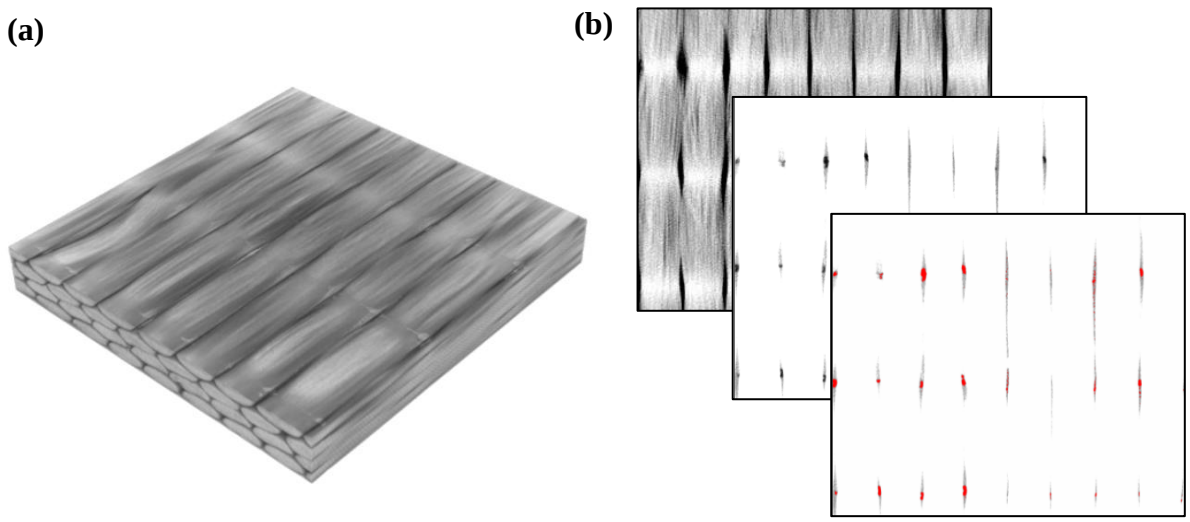

Figure 2: (a) Stacked 3D view of one of the 15mm x 15mm CT samples and (b) visual representation of the image processing steps used to analyse the void content and distribution.

2.5 Density determination and burn-off

The density of the 9 samples used for CT scans was determined in accordance with *ISO 1183-1 Method A: Immersion method* using Archimedes' principle by measuring the mass of each sample and its apparent mass in water. The samples were then heated in a furnace at 560°C for 5h to burn off the polymer matrix in accordance with *ISO 7822 Method A: Loss on ignition*. The weight loss was used to determine the fibre volume fraction. The burn-off and density data combined allowed for determination of the void content which could be compared with the CT values.

2.6 Flexural testing

All flexural samples were cut using a diamond blade and tested on an Instron 3369 screw-driven machine. The flexural extension was tracked at the mid-point of specimens using a video gauge in order to determine the strain and hence, modulus. For the pure polymer case, the samples were cut to 80mm x 10mm x 4mm and tested in three point bending in accordance with *BS EN 178:2010+A1:2013* using a span of 64mm. For the composite cases, 60mm x 15mm x 2mm specimens were cut and tested in four-point bending in accordance with *BS EN ISO 14125:1998+A1:2011* using a span of 45mm. A crosshead speed of 2mm/min. was used for the polymer specimens and 1mm/min. for composites. The composite samples were tested in both the transverse and longitudinal directions.

2.7 Scanning electron microscopy

The fracture surfaces of the 0° flexural specimens were observed using a JEOL JSM-6010PLUS/LV SEM. The samples were sputter coated with a 200Å layer of gold and were then viewed using an accelerating voltage of 20kV.

3 RESULTS

3.1 X-ray CT scanning

The scans show clearly how macro voids were formed in the material. In Figure 2 (b), the macro voids formed between bundles at the position of each stitch. Due to this effect, the transverse properties would likely be noticeably poorer in the inter-stitch regions due to a decrease in local cross sectional area. The cause of this occurrence was likely due to air/nitrogen gas in the mould which was ~6% by volume based on pressure readings during injection. While the resin pushed out most of the gas in front of the flow for the pure polymer case, the composite case was different as there was macro flow between fibre bundles and micro flow within bundles. A possible explanation of the macro-void stitch pattern is that while the macro flow moved forward, inter bundle flow followed, working its way from the bundle surface inward radially between fibres in the porous areas (areas between stitches) and then along the fibres longitudinally in both directions. It then likely got choked as it approached the stitch from both sides due to greater fibre compaction at the stitch and the gas in front was expelled in to the trenches between the bundles. In order to observe inter-bundle voids, it would be necessary to scan at a higher resolution over a much lower sample volume.

3.2 Density, fibre volume fraction and void content

The results for density measurements, fibre volume fraction and void content are summarised in Table 1 below. The density of the pure APA-6 is similar to that quoted in most literature [3], and it is a function of the amount of crystalline phase in the polymer. The density and fibre volume fraction measurements between the two composite cases are not too dissimilar, and the discrepancy between the two is due to slight variations in clamping pressure on the mould. Though the measured void content is relatively low, the burn-off method is only accurate to ± 2.5% by volume [15][16].

Plate	Density ρ (g/cm^3)	Fibre volume V_f (%)	Void volume V_v (%)
APA-6	1.147 ± 0.002	-	-
APA-6/GF871	1.883 ± 0.028	51.4 ± 2.0	0.8 ± 1.0
APA-6/GF886	1.906 ± 0.018	53.7 ± 1.0	1.3 ± 0.6

Table 1: Summarised results from density, fibre volume fraction and void volume fraction as determined from burn-off.

3.3 Flexural testing

The flexural test results are summarised in Table 2 below. The flexural strength and modulus values for the pure APA-6 polymer are in the range of those for standard hydrolytically polymerised PA-6 [17]. The pure polymer and transverse composite tests were discontinued after reaching maximum strength due to the increasingly large deflections, beyond which point, testing is no longer valid. The results show that the average transverse strength of the APA-6/GF886 composite samples is 21% higher than that of the APA-6/GF871 composites and 35.4% higher than the reported properties of organo-sheets

made from commercial UD GF/PA-6 tape [18]. The flexural modulus of the APA-6/GF886 is about 45% higher than those of the APA-6/GF871 and commercial organo sheet, while the strain-to-failure is slightly lower. Figure 3 is a visual representation of the stress-strain relationship in the transverse direction with the plot for the pure polymer added for comparison.

Significant improvements were also observed for the longitudinal (0°) composite properties by using the StarRov® 886 RXN rovings, where the strength was 23% higher than those of both the StarRov® 871 and the reported properties of the organo sheets [18]. The modulus was 46% higher than that of the StarRov® 871 and 22% higher than that of the organo sheet; albeit with a reduced strain-to-failure. Figure 4 is a visual representation of the stress-strain relationship in the longitudinal direction, which shows that for the most part, the relationship is linear but drops off slightly before sudden failure. The improved properties of the StarRov® 886 RXN composite with the functionalised sizing was expected due to the greater adhesion at the fibre-matrix interface. This radically reduces the degree of failure occurring at the interface which was the case for the StarRov® 871 as a result of poorer adhesion.

Test type	Maximum Strength (MPa)	Modulus (GPa)	Strain at maximum strength (%)
APA-6	102.7 ± 1.6	3.2 ± 0.2	6.2 ± 0.2
APA-6/GF871 (90°)	82.8 ± 9.8	10.3 ± 0.5	1.1 ± 0.1
APA-6/GF886 (90°)	100.4 ± 5.1	14.9 ± 0.7	0.9 ± 0.1
APA-6/GF871 (0°)	1158.2 ± 60.5	37.2 ± 3.0	3.0 ± 0.1
APA-6/GF886 (0°)	1370.0 ± 73.9	53.8 ± 3.6	2.4 ± 0.2

Table 2: Summarised results from density, fibre volume fraction and void volume fraction as determined from burn-off

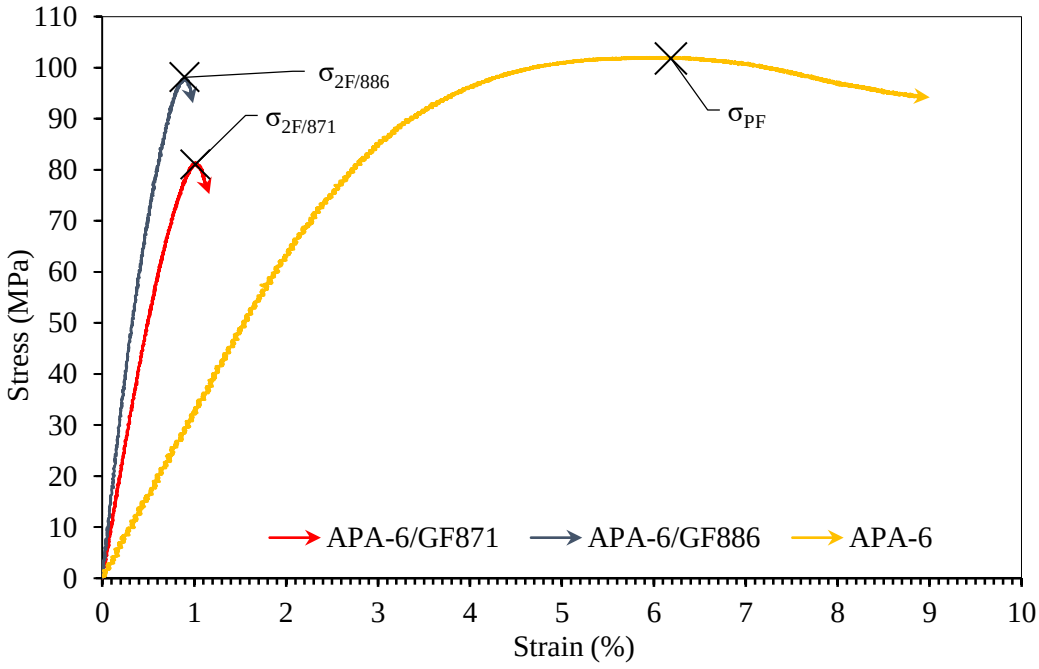

Figure 3: Typical representations of flexural test results for the pure APA-6 polymer and the composite in the transverse direction using StarRov® 871 and StarRov® 886 RXN.

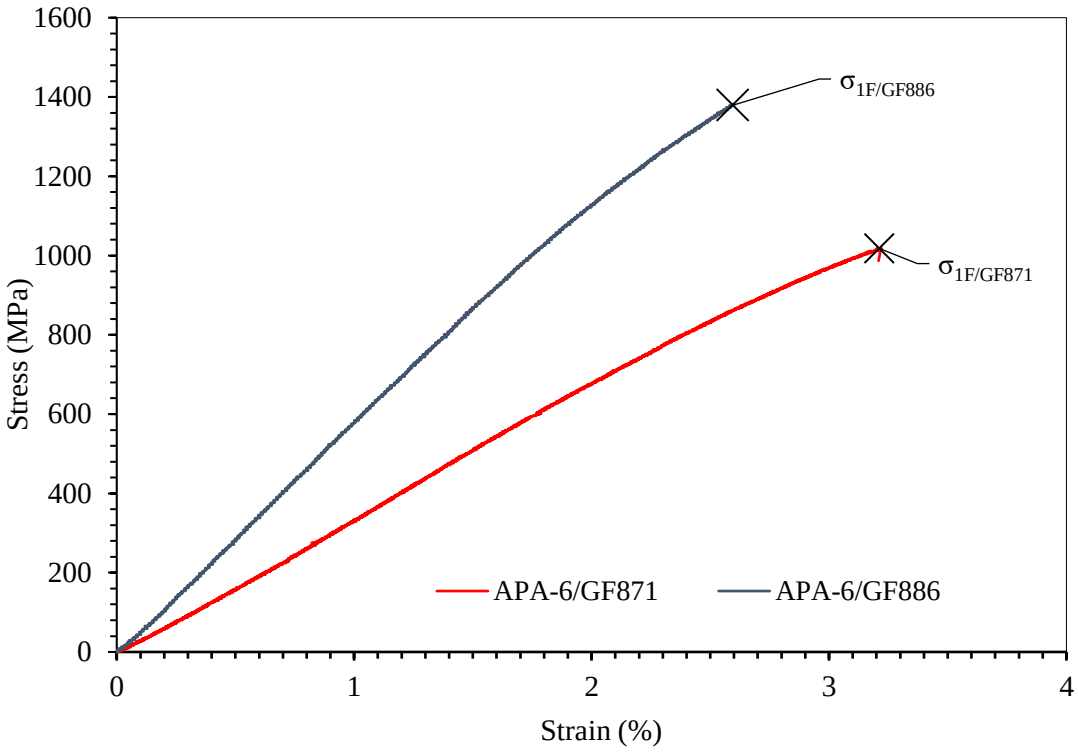

Figure 4: Typical plots of flexural test results for the composite in the longitudinal direction using StarRov® 871 and StarRov® 886 RXN.

3.4 Scanning electron microscopy

The SEM results showed clear differences between the two fibre sizing cases, and these were most visible in the section of the samples around the neutral axis of bending where the compressive and tensile regions meet due to the offset in the surface plane, which exposed the fibres. Figure 3 (a) and (b) are images of the composite made from the StarRov® 871 and (c) and (d) are images of the composite made from StarRov® 886 RXN. There is clearly better interfacial adhesion for the latter, where the failure seems to have been more matrix dominated. The images for the former show bare fibres, whereas those for the latter are heavily coated in polymer. Figure 3 (e) and (f) clearly demonstrate the ductile behavior of the APA-6 matrix in general.

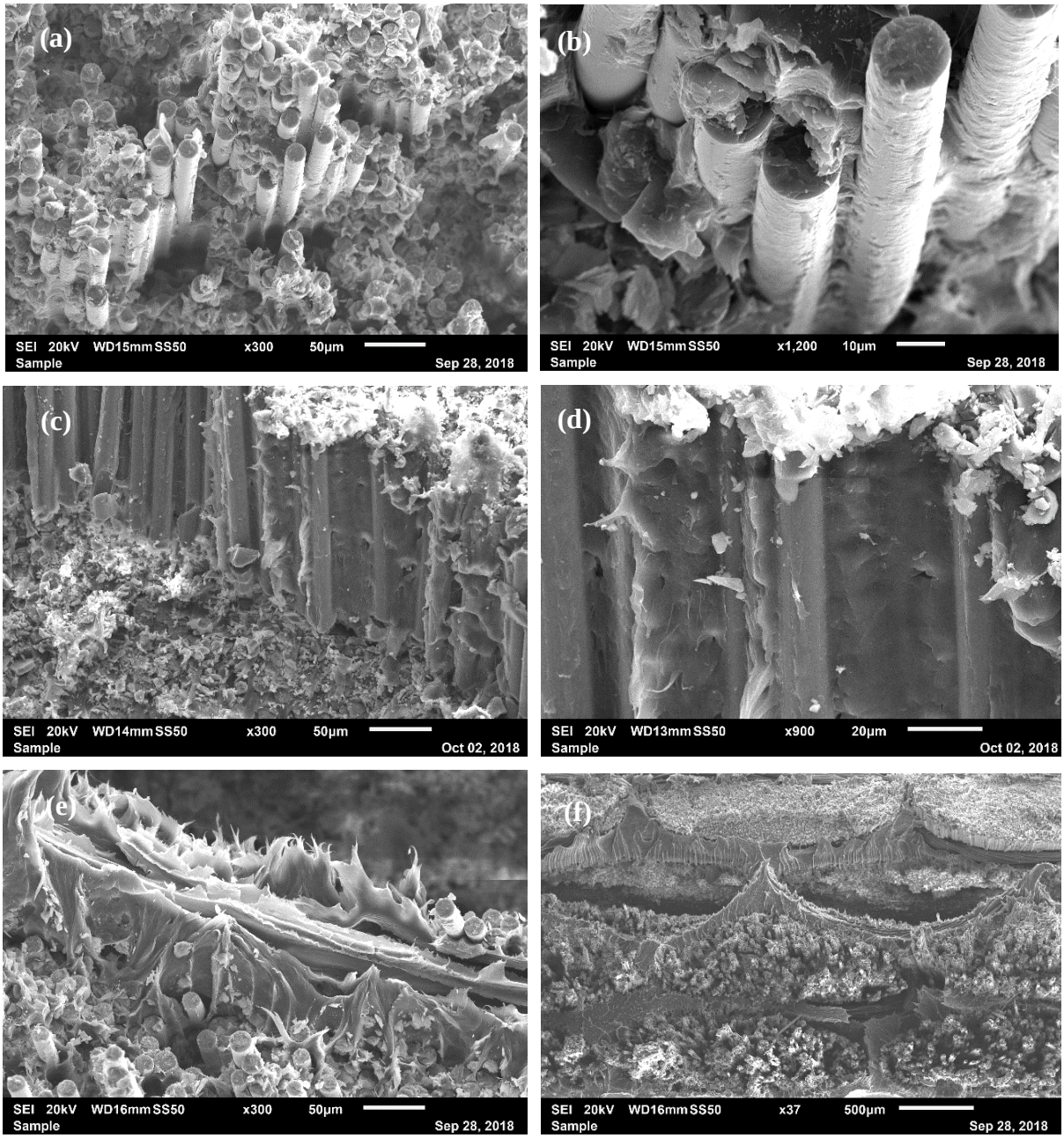

Figure 5: SEM images taken of the fracture surfaces of failed flexural specimens where (a) and (b) are images of StarRov® 871composites, (c) and (d) are images of StarRov® 886 RXN composites and (e) and (f) are images demonstrating the ductile nature of the polymer matrix.

4 CONCLUSIONS

This study shows that anionically polymerized PA-6 (APA-6) composites can be manufactured using inexpensive in-house built equipment to achieve high quality results. Composites with a fibre volume fraction of ~53% with a void volume of ~1% were achieved at pressures of only 4 bars. The results showed that significant improvements in flexural properties can be achieved by using functionalized sizings, which causes the bulk composite failure to occur in the matrix as opposed to the interface. This was confirmed by SEM. While the equipment is made to produce 350mm x 390mm laminates, there is no reason why this cannot be up-scaled by increasing the tank volume. Though moisture can cause problems with this polymerisation, it has been shown that if the correct procedures and equipment are used, the issue can be avoided. In order to further increase the speed of the whole process, a cooling system would be required but consideration should be given to the cooling rate through the crystallisation temperature range (153°C-173°C) such that polymer properties are tailored for the desired application. This could be further increased by using faster acting catalysts as well as automating the preform placement and part removal, similar to technologies which already exist for thermoset RTM processes. The ductile nature of the PA-6 matrix and the superior interface due to the sizing on the StarRov® 886 RXN would indicate that the composite toughness would be superior to most thermoset composites. An investigation of the fracture toughness and impact properties of this composite would be of interest to many industries prior to investing in such a system.

ACKNOWLEDGEMENTS

In addition to the authors mentioned, I would like to thank all the staff from Johns Manville who have co-funded this work and provided the fabrics used in the study. I would like to thank Brüggemann GmbH & Co. KG (Heilbronn, Germany) for kindly providing the caprolactam and all my colleagues and industrial partners who supported this work including Mr. Edward Monteith, Dr. Dimitrios Mamalis, Dr. James Maguire and Ms. Evanthia Pappa.

REFERENCES

[1] J. Summerscales, *Composites manufacturing for marine structures*. Elsevier Ltd., 2015.

[2] A. Murtagh, S. Coll, and C. Ó. Brádaigh, "Processing of Low-Viscosity Cbt Thermoplastic Composites : Heat Transfer," *Composites*, no. July, pp. 157–164, 2006.

[3] K. Van Rijswijk, J. J. E. Teuwen, H. E. N. Bersee, and a. Beukers, "Textile fiber-reinforced anionic polyamide-6 composites. Part I: The vacuum infusion process," *Compos. Part A Appl. Sci. Manuf.*, vol. 40, no. 1, pp. 1–10, 2009.

[4] W. Obande, D. Mamalis, D. Ray, L. Yang, and C. M. Ó Brádaigh, "Mechanical and thermomechanical characterisation of vacuum-infused thermoplastic- and thermoset-based composites," *Mater. Des.*, vol. 175, p. 107828, 2019.

[5] A. Luisier, P. Bourban, and J. Månson, "In Situ Polymerization of Polyamide 12 for Thermoplastic Composites," *Proc. ICCM-12, …*, 1999.

[6] H. Parton and I. Verpoest, "In situ polymerization of thermoplastic composites based on cyclic oligomers," *Polym. Compos.*, vol. 26, pp. 60–65, 2005.

[7] K. van Rijswijk, H. E. N. Bersee, W. F. Jager, and S. J. Picken, "Optimisation of anionic polyamide-6 for vacuum infusion of thermoplastic composites: choice of activator and initiator," *Compos. Part A*, vol. 37, pp. 949–956, 2006.

[8] K. van Rijswijk, a. a. van Geenen, and H. E. N. Bersee, "Textile fiber-reinforced anionic polyamide-6 composites. Part II: Investigation on interfacial bond formation by short beam shear test," *Compos. Part A Appl. Sci. Manuf.*, vol. 40, no. 8, pp. 1033–1043, 2009.

[9] K. van Rijswijk, H. E. N. Bersee, a. Beukers, S. J. Picken, and a. a. van Geenen, "Optimisation of anionic polyamide-6 for vacuum infusion of thermoplastic composites:

Influence of polymerisation temperature on matrix properties," *Polym. Test.*, vol. 25, no. 3, pp. 392–404, 2006.

[10] P. Seinsche, "T-RTM Components from Caprolactam – Performance Characteristics, Processing Aspects and In-line Testing, Employing Active Thermography," in *SAMPE Europe*, 2017, pp. 1–8.

[11] S. Schmidhuber and P. Zimmermann, "It Couldn't Be More Hybrid. Thermoplastic-Matrix RTM on the Roof Frame of the Roding Roadster," *Kunstst. Intl.*, no. 1–2, pp. 36–38, 2017.

[12] M. Bitterlich, "Tailored to Reactive Polyamide 6: Thermoplastic Resin Transfer Moulding," pp. 47–51, 2014.

[13] T. Ageyeva, I. Sibikin, and J. Karger-Kocsis, "Polymers and related composites via anionic ring-opening polymerization of lactams: Recent developments and future trends," *Polymers*, vol. 10, no. 4. 2018.

[14] W. V Steele, R. D. Chirico, S. E. Knipmeyer, A. Nguyen, B. D. M. P. Technologies, and P. O. Box, "Measurements of Vapor Pressure, Heat Capacity, and Density along the Saturation Line for E-Caprolactam, Pyrazine, 1,2-Propanediol, Triethylene Glycol, Phenyl Acetylene, and Diphenyl Acetylene," *J. Chem. Eng.*, vol. 47, pp. 689–699, 2008.

[15] British Standards Institution, "BS EN ISO 7822-1999," 1999.

[16] B. S. W. Lye, "Void reduction in autoclave processing of thermoset composites," vol. 23, no. 4, pp. 261–265, 1992.

[17] M. Xenopoulos, A and Clark, ES and Kohan, "Nylon plastics handbook," *Kohan, MI, Ed*, vol. 1, no. 3, p. 108, 1995.

[18] SGL Group, "Unidirectional glass fiber tape with thermoplastic matrix datasheet." 2017.